

# Microelectromechanical control of the state of quantum cascade laser frequency combs

Cite as: Appl. Phys. Lett. **115**, 021105 (2019); <https://doi.org/10.1063/1.5098086>

Submitted: 31 March 2019 . Accepted: 24 June 2019 . Published Online: 11 July 2019

David Burghoff, Ningren Han, Filippas Kapsalidis , Nathan Henry, Mattias Beck , Jacob Khurgin , Jerome Faist , and Qing Hu



View Online



Export Citation



CrossMark



**THE WORLD'S RESOURCE FOR  
VARIABLE TEMPERATURE  
SOLID STATE CHARACTERIZATION**



[WWW.MMR-TECH.COM](http://WWW.MMR-TECH.COM)

OPTICAL STUDIES SYSTEMS

SEEBECK STUDIES SYSTEMS

MICROPROBE STATIONS

HALL EFFECT STUDY SYSTEMS AND MAGNETS



# Microelectromechanical control of the state of quantum cascade laser frequency combs

Cite as: Appl. Phys. Lett. **115**, 021105 (2019); doi: [10.1063/1.5098086](https://doi.org/10.1063/1.5098086)

Submitted: 31 March 2019 · Accepted: 24 June 2019 ·

Published Online: 11 July 2019



View Online



Export Citation



CrossMark

David Burghoff,<sup>1,2,a)</sup> Ningren Han,<sup>1</sup> Filippos Kapsalidis,<sup>3</sup>  Nathan Henry,<sup>4</sup> Mattias Beck,<sup>3</sup>  Jacob Khurgin,<sup>4</sup>   
Jerome Faist,<sup>3</sup>  and Qing Hu<sup>1</sup>

## AFFILIATIONS

<sup>1</sup>Department of Electrical Engineering and Computer Science, Research Laboratory of Electronics, Massachusetts Institute of Technology, Cambridge, Massachusetts 02139, USA

<sup>2</sup>Department of Electrical Engineering, University of Notre Dame, Notre Dame, Indiana 46556, USA

<sup>3</sup>Institute for Quantum Electronics, ETH Zurich, Zurich CH-8093, Switzerland

<sup>4</sup>Department of Electrical and Computer Engineering, Johns Hopkins University, Baltimore, Maryland 21218, USA

<sup>a)</sup>Electronic mail: [dburghoff@nd.edu](mailto:dburghoff@nd.edu)

## ABSTRACT

Chip-scale frequency combs such as those based on quantum cascade lasers (QCLs) or microresonators are attracting tremendous attention because of their potential to solve key challenges in sensing and metrology. Though nonlinearity and proper dispersion engineering can create a comb—light whose lines are perfectly evenly spaced—these devices can enter into different states depending on their history, a critical problem that can necessitate slow and manual intervention. Moreover, their large repetition rates are problematic for applications such as dual comb molecular spectroscopy, requiring gapless tuning of the offset. Here, we show that by blending midinfrared QCL combs with microelectromechanical comb drives, one can directly manipulate the dynamics of the comb and identify new physical effects. Not only do the resulting devices remain on a chip-scale and are able to stably tune over large frequency ranges, but they can also switch between different comb states at extremely high speeds. We use these devices to probe hysteresis in comb formation and develop a protocol for achieving a particular comb state regardless of its initial state.

Published under license by AIP Publishing. <https://doi.org/10.1063/1.5098086>

Chip-scale frequency combs are expected to have an enormous impact in the area of sensing, as their properties give them unique abilities in spectroscopy and ranging.<sup>1</sup> In particular, quantum cascade laser (QCL) combs<sup>2–4</sup> operating in the midinfrared and terahertz regions offer the ability to perform sensing in the highly relevant “molecular fingerprint” ranges, where many molecules relative to chemical and biological sensing have fundamental rovibrational transitions.<sup>5–7</sup> Nonetheless, one challenge associated with these devices is that even with proper dispersion engineering,<sup>3,8–11</sup> the spatial hole burning (SHB) mechanism that enables comb formation<sup>12</sup> sometimes allows for multiple types of comb states to form. Although the combs are extremely “reproducible”—turning the comb on the same way always leads it to a definite state<sup>13</sup>—under usage conditions, they are frequently “multistable,” entering into different states based on their history. For example, one may access a particular state if the laser is simply turned on, but a different one by ramping the current up and back down. One could also destroy the comb state with optical feedback.<sup>14</sup> A variety of states arise from the fact that the internal dynamics of QCLs attempt to maximize the average round trip gain of the laser by

making use of SHB, which allows more than one mode to lase.<sup>15,16</sup> However, even in the absence of dispersion, the energy landscape of SHB is highly nonmonotonic, possessing a small number of local maxima with similar round trip gains. These are locally stable, allowing them to be used in applications like dual-comb spectroscopy, but perturbations can still cause them to jump between regimes. Unfortunately, accessing and controlling these states are difficult using conventional tuning schemes, such as changing the gain medium’s bias and temperature. One way to modify the properties of a QCL comb without contact is to put an object near the facet, changing the intracavity dispersion.<sup>17</sup> In principle, it also changes the mode profile and the SHB pattern of the cavity—allowing different states to be accessed—although it does so relatively slowly and at the cost of making the device no longer on a chip-scale.

In order to access these states, here we quasi-integrate a microelectromechanical (MEMS) comb drive alongside a QCL frequency comb. The resulting device is still on the chip-scale, but by blending it with a mirror whose position can be quickly modulated electrically, we can repeatedly probe and access different comb states. In addition,

because this device has a submillisecond response time, it is suitable for use in feedback configurations where either the repetition or the offset frequency of the comb needs to be stabilized. This allows the offset frequency of the laser to be tuned gaplessly with a repetition rate that is stable (i.e., acquiring spectra continuously between discrete comb lines), or allows the repetition rate to be tuned, as the offset remains stable. A schematic of our devices is shown in Fig. 1(a). The lasers themselves are conventional midinfrared QCLs at  $7.8\ \mu\text{m}$  without any dispersion management; details of the gain medium can be found in Ref. 18. They are  $6\ \mu\text{m}$  wide,  $6\ \text{mm}$  long, mounted epi-layer down on AlN submounts, have a threshold current of about  $0.8\ \text{A}$ , and begin to enter multimode regimes beyond  $1.75\ \text{A}$ . The MEMS comb drive was designed for tuning QCLs and was fabricated in a commercial foundry (MEMSCAP Inc.) that utilized a silicon-on-insulator (SOI)-based process.<sup>19</sup> The tuner mirror is  $800\ \mu\text{m}$  wide by  $25\ \mu\text{m}$  tall, the chip is  $4\ \text{mm}$  across, and by applying a voltage between  $0$  and  $50\ \text{V}$  to the comb drive, the position of the tuner can be modulated by up to  $10\ \mu\text{m}$ . For all measurements but the one shown in Fig. 1(b), the MEMS chips were bonded to the AlN submount of the QCL.

To show that the MEMS is able to effectively modulate the dispersion despite its narrow cross section, we affixed a tuner to a computer-controlled stage and recorded the repetition rate beatnote measured on a high-speed quantum well infrared photodetector (QWIP), shown in Fig. 1(b). (The lateral and transverse

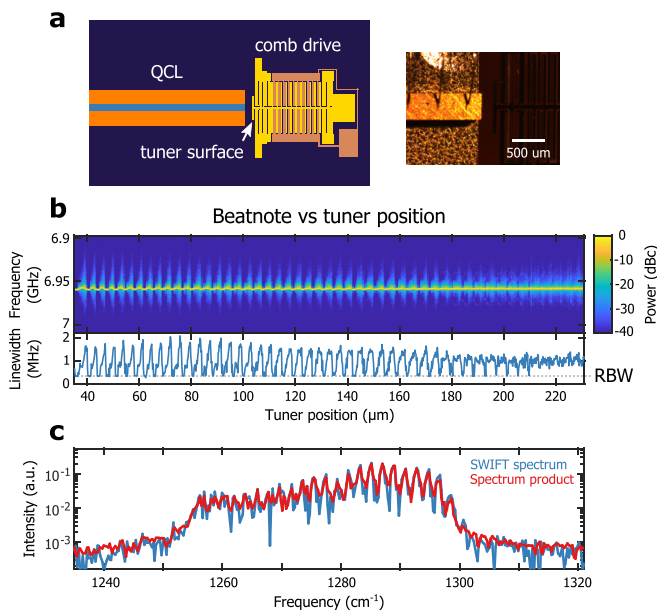


**FIG. 1.** Basic properties of a MEMS-actuated comb. (a) Schematic and picture of a MEMS-actuated comb. (b) Beatnote map of a comb measured on a QWIP, as the MEMS tuner is scanned over a long distance, along with the standard deviation linewidth. As the tuner is scanned, the dispersion is modulated periodically, causing the device to shift between narrow and broad beatnote regimes. [The linewidth of narrow beatnote regimes is far narrower than the resolution bandwidth (RBW), so this is the minimum value observed.] Far from the laser, the effect is too small and the beatnote remains broad. (c) SWIFTS measurement of the laser in a narrow beatnote regime. The SWIFTS signal matches the spectrum product, proving comb operation. Each marker represents one mode; the etalon effect comes from a  $775\ \mu\text{m}$  Si beam splitter that was used to sample the beam.

alignments were ensured using a microscope, but were not found to be critical.) As the tuner is moved away from the QCL, the dispersion is modulated periodically, causing the device to shift between narrow and broad beatnote regimes. As expected, this periodicity is half the wavelength.<sup>17</sup> Far from the laser, however, the effect is too small as very little light couples back into the cavity. As a result, the beatnote remains broad, and this device is unable to form a comb at this bias without the dispersion compensation added by the tuner. Note that in comb regimes, the beatnote linewidth falls well below the resolution bandwidth (RBW) of Fig. 1(b). Therefore, to prove that the laser is truly operating as a comb in these narrow beatnote regimes, we fix the position of the tuner, lock the beatnote to a local oscillator, and perform a SWIFTS measurement<sup>3,13,14</sup> to assess the equidistance, shown in Fig. 1(c). The close agreement between the SWIFT spectrum and the spectrum product— $|\langle E^*(\omega)E(\omega + \omega_{LO}) \rangle|$  and  $\sqrt{\langle |E(\omega)|^2 \rangle \langle |E(\omega + \omega_{LO})|^2 \rangle}$ , respectively—shows that the laser is a comb that is coherent across its bandwidth.

Next, we fixed the MEMS's position and show that the comb drive is capable of fully adjusting the state of the QCL comb. For Figs. 2–4, the MEMS chip was bonded directly to the QCL submount using optical adhesive, ensuring that the system is mutually stable and compact. Because the dispersion induced by the tuner is approximately periodic in half the wavelength, as long as the comb drive is able to cover this distance the precise positioning of the MEMS structure does not matter (provided it is close enough to ensure sufficient coupling with the laser). We chose to bond the MEMS at a distance of  $150\ \mu\text{m}$  from the laser, close enough to provide enough dispersion compensation to enable

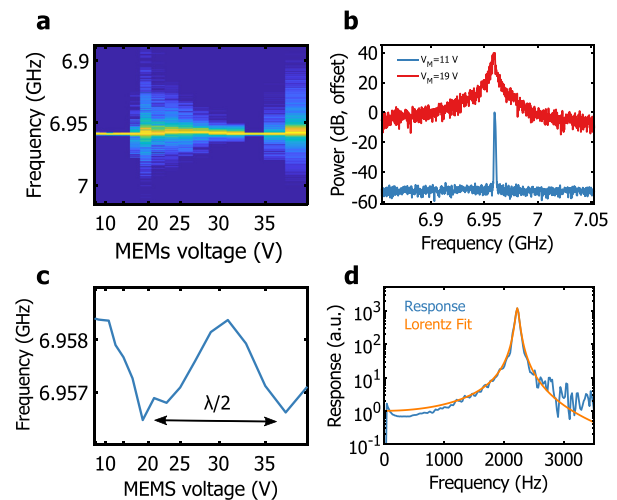


**FIG. 2.** Properties of the MEMS tuner. (a) Beatnote map of the comb measured on a QWIP as a function of MEMS voltage. [Colors identical to Fig. 1(b).] More than one period of Fig. 1(b) is accessible. (b) Beatnotes under a bias of  $11\ \text{V}$  and  $19\ \text{V}$ , showing that both comb and broad beatnote states are accessible. (c) Beatnote mean frequency as a function of MEMS voltage. The voltage is plotted on a quadratic scale since displacement is proportional to  $V^2$ . (d) Top: step response of the MEMS tuner as assessed by small-signal modulation of the QCL. Bottom: calculated response, showing a resonant frequency of  $2.2\ \text{kHz}$  and a response speed of about  $3\ \text{kHz}$ .

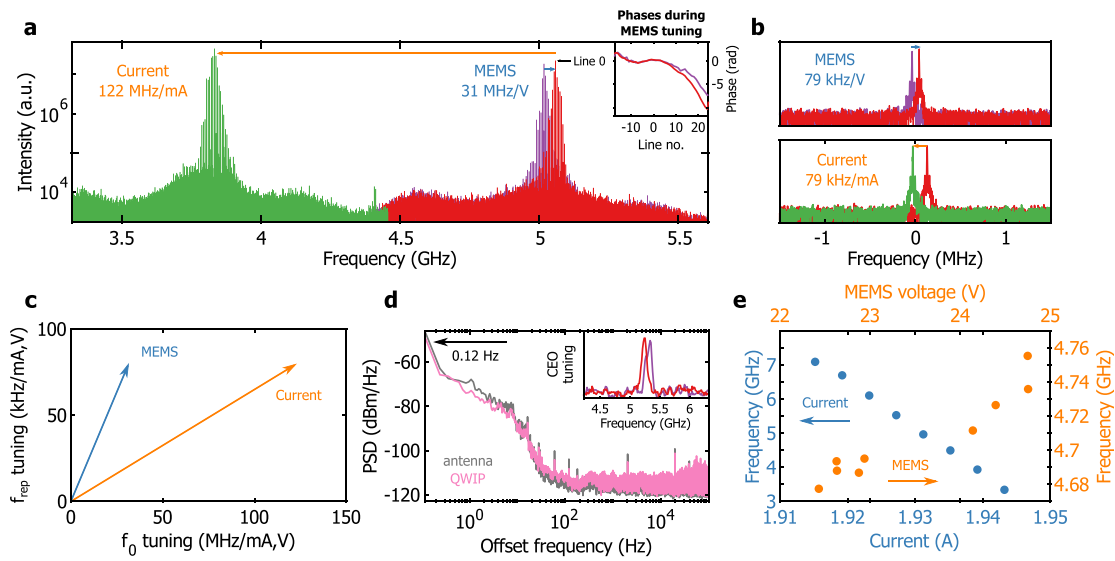


**FIG. 3.** Tuning of the QCL comb. (a) Results of a dual comb measurement used to measure tuning coefficients. The purple curve is the dual comb spectrum before any adjustment, the red curve is the spectrum following a MEMS adjustment, and the green curve is the spectrum following a subsequent current adjustment. Inset: Dual comb phases during MEMS tuning. Due to the modified dispersion, additional chirp is apparent. (b) Beatnote shifts following a MEMS adjustment (top) and following a current adjustment (bottom), offset from 6.93 GHz. (c) Tuning vectors for current and MEMS tuning. Though they are not orthogonal, they are linearly independent. (d) Stabilization of the repetition rate to subhertz levels using the beatnote measured by an antenna near the laser. This also stabilizes the QWIP beatnote. Inset: Offset tuning with a stabilized beatnote (with a RBW of 56 MHz, so lines are not resolved). (e) Offset tuning via current and via MEMS. Current tuning can provide gapless tuning (more than the  $\text{FSR}/2 = 3.95$  GHz).

comb operation, but far enough to prevent the laser from slowly overheating and burning the tuner. The MEMS voltage was then swept and the beatnote on the QWIP was recorded; the result is shown in Fig. 2(a). Once again, we find that the beatnote oscillates between the comb and broad beatnote regimes in a nearly periodic way; however, only two periods are covered over the MEMS sweeping range. Comparing Fig. 2(a) and Fig. 1(b), we can also note that the shape of the dependence is horizontally flipped, as the electrostatic force is attractive and pulls the tuner toward the QCL; moreover, since the displacement of the tuner is proportional to the squared voltage, the map must be plotted on a quadratic scale to appear periodic. Figure 2(c) shows the center frequency of each beatnote as a function of MEMS voltage; by extracting the periodicity, we infer a coefficient of proportionality of  $3.9 \text{ nm}/\text{V}^2$ . Figure 2(c) can also be used to measure the group delay dispersion (GDD) introduced by the MEMS, since the beatnote center frequency is the inverse of the cavity group delay. By comparing the maximum and minimum group delays (which differ by 40 fs), one finds that the MEMS is capable of adding or removing approximately  $20\,000 \text{ fs}^2$  of dispersion. Lastly, we used the QCL to optically measure the response speed of the comb drive. To do this, we biased the laser to a single-mode regime (1.08 A) and examined the step response of the QWIP signal for a small step applied to the MEMS voltage. By comparing the QWIP signal to the drive voltage—as shown in Fig. 2(d)—one finds that the MEMS has a response of up to about 3 kHz and a resonant frequency of 2.2 kHz. This fast response makes it suitable for use in feedback configurations.

In order to assess the efficacy of the MEMS tuners and to show their suitability for gapless dual comb spectroscopy, we performed a series of dual comb measurements to measure the tuning coefficients of the MEMS voltage and the current. A QCL with a MEMS tuner was

beat against a QCL with a planar mirror tuner<sup>17</sup> on the QWIP, and the multiheterodyne beating was recorded. Figure 3(a) shows some of these measurements. First, the MEMS voltage was tuned, resulting in a dual-comb offset frequency measurement. Next, the current through the device was tuned, giving a tuning coefficient of 122 MHz/mA. Figure 3(b) shows the corresponding effects on the laser's beatnote (repetition rate), giving tuning coefficients of 79 kHz/V and 79 kHz/mA, respectively. Evidently, both the current and the MEMS voltage affect both the repetition rate and offset. Although the shift of the offset is much larger numerically than that of the repetition rate in both cases, this is primarily because offset shifts are expected to be on the order of  $N$  times larger than repetition rate shifts, where  $N$  is the number of comb lines. Still, there is a large “relative” difference in current tuning and MEMS tuning; perturbations that result in the same shift of the repetition rate give rise to an offset shift that is four times larger in the case of current tuning. The physical origin of this effect is that the MEMS position primarily acts by changing the end of the cavity, thereby changing its “group delay,” whereas current primarily acts by changing the refractive index “along” the cavity, thereby changing its carrier offset. Nevertheless, these tuning directions are linearly independent in phase space—see Fig. 3(c)—which means that it is possible to use one parameter to stabilize the repetition rate and another parameter to tune the offset frequency. Although computational phase correction<sup>20–22</sup> makes it possible to analyze dual comb data in the absence of repetition rate stabilization, stabilization makes it possible to make  $\Delta f_{\text{rep}}$  arbitrarily small, significantly reducing the bandwidth requirements of the sampling electronics. It also ensures that the laser will not exit the comb regime due to feedback or mechanical vibrations, making the comb more robust. Figure 3(d) plots an example of such stabilization: by using one parameter to lock the beatnote to a

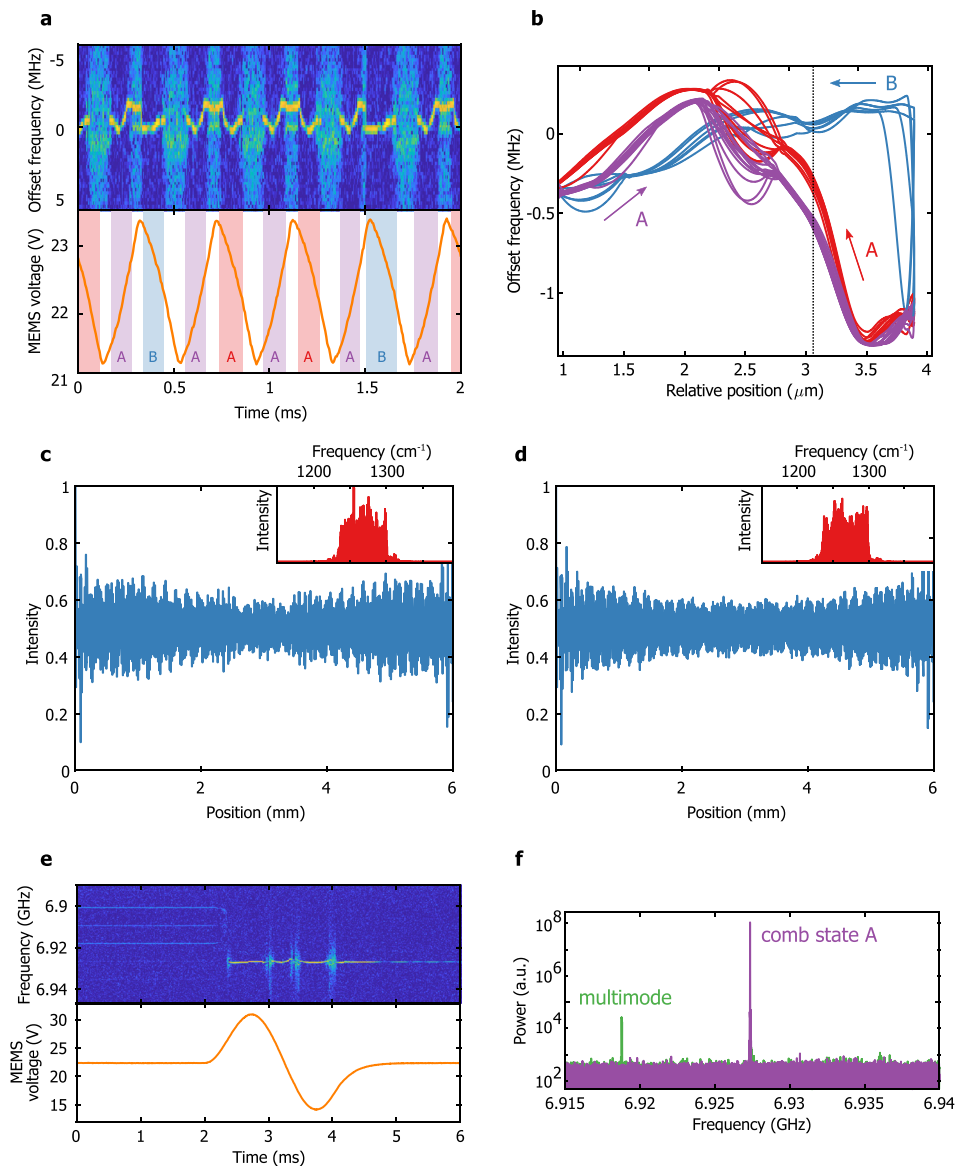


**FIG. 4.** Control of the comb state. (a) Top: Beatnote map as the MEMS tuner is quickly modulated, demonstrating access to multiple comb states. Bottom: Corresponding MEMS voltage, with different comb states highlighted. Purple indicates state A with increasing voltage, red indicates state A with decreasing voltage, and blue represents state B with decreasing voltage. (State B is never observed with increasing voltage.) (b) Phase space plot of the offset frequency vs MEMS position. At the bifurcation point ( $3.9 \mu\text{m}$ ), the laser can enter either state A or state B. (c) and (d) Simulated intensity profiles (main) and the corresponding spectra (inset) of two states that maximize the round trip gain of the laser. They are qualitatively similar, but quantitatively distinct. (e) Beatnote map of a multimode state (top) converted into a comb state by the application of a MEMS voltage pulse (bottom). (f) Beatnotes before and after the voltage pulse. Note that the beatnote of a comb state is much larger than that of a multimode state, on account of the fact that it contains many more modes.

synthesizer, and the linewidth measured on the QWIP can be made extremely narrow, even subhertz. Then, as the other parameter is changed, the offset frequency of the comb shifts [as seen in the inset of Fig. 3(d)], as the repetition rate is forced to remain stable. Note that because current tuning is monotonic, while MEMS tuning is periodic, it is possible to tune the offset much farther with current than with MEMS [see Fig. 3(e)]. Current tuning allows for gapless tuning of several free spectral ranges (FSRs), which means that for stabilized gapless spectroscopy one should stabilize and tune the offset with current, while using MEMS to stabilize the beatnote.

Finally, we show that it is possible to use the MEMS tuner to controllably access different comb states on short timescales. As previously noted, QCL combs can possess a number of different states that can be accessed depending on how their history and measurements such as the ones in Figs. 1(b) and 2(a) were performed in a pulsed mode with

long pulses ( $10 \mu\text{s}$ ) to be repeatable. However, in a continuous wave mode, such plots are misleading, because the comb can enter multiple states depending on whether they were turned on from zero bias, turned on from a high bias and then decreased, had their comb operation destroyed by feedback, etc. To characterize this effect in a controllable way requires fast modulation of the laser parameters, but even current tuning can be slow as it induces an indirect temperature shift that takes seconds for a controller to recover from. Modulating the MEMS tuner has no such constraints, so in Fig. 4(a), we modulate the MEMS voltage at  $2.5 \text{ kHz}$ —close to its resonant frequency—and examine the beatnote. At low MEMS voltages, the laser is in a broad beatnote regime. As the voltage is increased, the laser always enters a comb regime where the beatnote initially falls and then rises (state A, denoted by purple stripes). At high voltages, it enters another broad beatnote regime. As the voltage is now decreased, one of two things

can happen: either the beatnote frequency immediately jumps to a higher frequency (state B, denoted by blue), or it reenters state A (denoted by red). By plotting the frequency as a function of MEMS position [Fig. 4(b)], this hysteresis is made more explicit. The purple curves indicate increasing distance from the laser; all of the curves overlay because the comb always enters state A from the low-bias broad beatnote regime. However, as the voltage hits its peak distance, the purple curves bifurcate, with some following the red path (state A) and some following the blue path (state B). A possible interpretation for this apparent randomness is that when the tuner is the furthest from the laser, it quickly switches between the two states, only settling in one or the other when brought closer. “Both” the red paths and the blue paths represent stable comb states, and even though all of the parameters are the same—dispersion, current, temperature, and optical feedback—they have different optical spectra, different phases, and different beatnotes. This bistability arises because SHB is highly non-monotonic, allowing the laser to settle into different local maxima of the energy landscape. An example of two intensity profiles that minimize the gain of the laser are simulated in Figs. 4(c) and 4(e), along with the corresponding spectra. Though they are qualitatively similar, they nonetheless possess quantitative differences. Accessing these different states with current and temperature is an extremely slow process, but accessing them with MEMS takes only milliseconds. If the comb is destroyed with feedback, this laser also has the ability to enter a multimode regime, where no comb is formed and only a few modes lase [Fig. 4(f)]. Nonetheless, we show in Fig. 4(e) how the laser can always be brought into state A: by adding a positive pulse to the MEMS voltage, the laser enters states A or B, and then by adding a negative pulse to the MEMS voltage, it always enters state A. Although state B cannot be accessed as reliably—a positive pulse can select either state A or B—if one wanted to reliably enter state B, one would only have to serially add positive pulses until the correct state was selected. (The relative difficulty in accessing state B suggests that it is the higher-energy of the two states.)

In conclusion, we have shown that a MEMS comb drive can be used to control the state of chip-scale frequency combs such as those based on quantum cascade lasers. This approach does not substantially increase the size of the devices, and can be used to select a particular comb state when more than one is possible. In addition, it can be used to simultaneously stabilize and tune both the offset frequency and the repetition rate, an important task for applications requiring reliable gapless spectroscopy. Finally, we note that the high power of mid-IR QCLs creates a non-negligible photon pressure of light on the MEMS surface, and while the resulting displacement is too small to be of interest in this case ( $\sim 1$  nm), these types of systems still have the potential to create interesting cavity optomechanical devices at mid-IR frequencies.

The work was supported by the Defense Advanced Research Projects Agency (DARPA) and the U.S. Army Aviation and Missile Research, Development, and Engineering Center (AMRDEC) through Grant No. W31P4Q-16-1-0001. The views and conclusions contained in this document are those of the authors and should not be interpreted as representing the official policies, either expressed or implied, of the Defense Advanced Research Projects Agency, the U.S. Army, or the U.S. Government.

D.B. was supported by the Intelligence Community Postdoctoral Research Fellowship Program at MIT, administered by Oak Ridge Institute for Science and Education through an interagency agreement between the U.S. DOE and the Office of the Director of National Intelligence.

## REFERENCES

- <sup>1</sup>P. Trocha, M. Karpov, D. Ganin, M. H. P. Pfeiffer, A. Korde, S. Wolf, J. Krockenberger, P. Marin-Palomo, C. Weimann, S. Randel, W. Freude, T. J. Kippenberg, and C. Koos, *Science* **359**, 887 (2018).
- <sup>2</sup>A. Hugi, G. Villares, S. Blaser, H. C. Liu, and J. Faist, *Nature* **492**, 229 (2012).
- <sup>3</sup>D. Burghoff, T.-Y. Kao, N. Han, C. W. I. Chan, X. Cai, Y. Yang, D. J. Hayton, J.-R. Gao, J. L. Reno, and Q. Hu, *Nat. Photonics* **8**, 462 (2014).
- <sup>4</sup>M. Rösch, G. Scalari, M. Beck, and J. Faist, *Nat. Photonics* **9**, 42 (2015).
- <sup>5</sup>A. R. Wilmsmeyer, W. O. Gordon, E. D. Davis, D. Troya, B. A. Mantooth, T. A. Lalain, and J. R. Morris, *J. Phys. Chem. C* **117**, 15685 (2013).
- <sup>6</sup>J. Westberg, L. A. Sterczewski, F. Kapsalidis, Y. Bidaux, J. Wolf, M. Beck, J. Faist, and G. Wysocki, in *Conference on Lasers and Electro-Optics (OSA, Washington, D.C., 2018)*, p. STh1L.5.
- <sup>7</sup>L. A. Sterczewski, J. Westberg, Y. Yang, D. Burghoff, J. Reno, Q. Hu, and G. Wysocki, *Optica* **6**, 766 (2019).
- <sup>8</sup>G. Villares, S. Riedi, J. Wolf, D. Kazakov, M. J. Süess, P. Jouy, M. Beck, and J. Faist, *Optica* **3**, 252 (2016).
- <sup>9</sup>Y. Bidaux, I. Sergachev, W. Wuester, R. Maulini, T. Gresch, A. Bismuto, S. Blaser, A. Müller, and J. Faist, *Opt. Lett.* **42**, 1604 (2017).
- <sup>10</sup>D. Burghoff, Y. Yang, J. L. Reno, and Q. Hu, *Optica* **3**, 1362 (2016).
- <sup>11</sup>Y. Yang, D. Burghoff, J. Reno, and Q. Hu, *Opt. Lett.* **42**, 3888 (2017).
- <sup>12</sup>J. B. Khurgin, Y. Dikmelik, A. Hugi, and J. Faist, *Appl. Phys. Lett.* **104**, 081118 (2014).
- <sup>13</sup>M. Singleton, P. Jouy, M. Beck, and J. Faist, *Optica* **5**, 948 (2018).
- <sup>14</sup>D. Burghoff, Y. Yang, D. J. Hayton, J.-R. Gao, J. L. Reno, and Q. Hu, *Opt. Express* **23**, 1190 (2015).
- <sup>15</sup>N. Henry, D. Burghoff, Y. Yang, Q. Hu, and J. B. Khurgin, *Opt. Eng.* **57**, 011009 (2017).
- <sup>16</sup>N. Henry, D. Burghoff, Q. Hu, and J. B. Khurgin, *Opt. Express* **26**, 14201 (2018).
- <sup>17</sup>J. Hillbrand, P. Jouy, M. Beck, and J. Faist, *Opt. Lett.* **43**, 1746 (2018).
- <sup>18</sup>F. Kapsalidis, M. Shahmohammadi, M. J. Süess, J. M. Wolf, E. Gini, M. Beck, M. Hundt, B. Tuzson, L. Emmenegger, and J. Faist, *Appl. Phys. B* **124**, 107 (2018).
- <sup>19</sup>N. Han, A. de Geofroy, D. P. Burghoff, C. W. I. Chan, A. W. M. Lee, J. L. Reno, and Q. Hu, *Opt. Lett.* **39**, 3480 (2014).
- <sup>20</sup>D. Burghoff, Y. Yang, and Q. Hu, *Sci. Adv.* **2**, e1601227 (2016).
- <sup>21</sup>L. A. Sterczewski, J. Westberg, and G. Wysocki, “Computational coherent averaging for free-running dual-comb spectroscopy,” preprint arXiv (2018).
- <sup>22</sup>N. B. Hébert, J. Genest, J.-D. Deschênes, H. Bergeron, G. Y. Chen, C. Khurmi, and D. G. Lancaster, *Opt. Express* **25**, 8168 (2017).